High Sensitivity Differential Phase OTDR for Acoustic Signals Detection

Wendy Tomboza, Sterenn Guerrier, Elie Awwad, *Member, IEEE,* and Christian Dorize

***Abstract*—We demonstrate the detection of speech signals and footsteps through a novel polarization-multiplexed coded differential-phase OTDR (optical time domain reflectometry) interrogation of standard telecom fibers in different configurations. We assess the sensitivity to audio signals by measuring the induced phase variation with respect to the sound pressure level of the perturbation, and manage to detect acoustic signals with high reliability. Further experiments are performed using an installed fiber cable showing the ability to track footsteps in an indoor scenario. These experiments pave the way for numerous applications of Distributed Acoustic Sensing (DAS) where a high sensitivity is required.**

***Index Terms*—Optical fiber sensors, $\Delta\Phi$-OTDR, Rayleigh scattering, Distributed acoustic sensing.**

I. Introduction

DISTRIBUTED Acoustic Sensing (DAS) meets a growing interest in monitoring since we can use optical fibers as distributed microphones, as demonstrated in [1], [2]. Optical fiber sensors have attractive characteristics such as wide bandwidth and immunity to electromagnetic interference [3], which make them more suitable than other more conventional sensors such as electronic, piezoelectric or micro-electro-mechanical systems (MEMS) devices. The large amount of fibers already deployed for telecom transmission in urban regions makes possible the implementation of new sensing and monitoring features, in order to create safer and smarter urban environments. Recent progress in DAS schemes including the exploitation of the phase information of the backscattered signal [4]–[6], instead of the sole intensity, offers better sensitivity and linearity, and allows identification of complex mechanical and acoustical events with larger bandwidth and dynamic range. In addition, we have recently proposed a new MIMO (Multiple-Input-Multiple Output) interrogation technique based on coherent differential-phase OTDR with polarization multiplexing of two probing sequences at the transmitter and polarization diversity detection at the coherent receiver. This method offers an enhanced sensitivity compared to single-pulse single-polarization coherent DAS [7], [8]. The ability of our interrogation technique to detect mechanical events over a 50km standard single mode fiber (SSMF) by using a piezoelectric actuator as a mechanical perturbation was shown in [9] as well as a preliminary demonstration of the detection of acoustic perturbations in [10].

In this paper, we characterize the sensitivity and the reliability of our new technique when acoustic perturbations of various level and nature are applied to the fiber. We first demonstrate the ability to detect acoustic events through a speaker located at 30cm in front of a 1mm tight buffered SSMF. We describe the physical configuration of the fiber and its isolation environment, and we emphasize on their impact on the detected acoustic signals. We demonstrate the detection of a speech signal with a mean squared error (MSE) close to 3%. Finally, we highlight the detection of anthropogenic activity through an underground installed fiber cable.

The authors are/were with Nokia Bell Labs France, route de Villejust, 91620 Nozay. W. Tomboza is now with Safran Group and E. Awwad is now with Télécom Paris, IP Paris. E-mail addresses: wendy.tomboza@safrangroup.com, {sterenn.guerrier ,christian.dorize}@nokia-bell-labs.com, elie.awwad@telecom-paris.fr.

First version received April 22, 2020, revised version received March 11, 2021.

II. Fiber response estimation with polarization multiplexed code

A. Probing method

In current DAS systems, the transmitter sends periodic pulses on a single polarization axis, generated by a narrow linewidth laser, along with a direct or coherent detection based receiver. The main limitations of these schemes are coherent fading (speckle pattern in back-scattered intensity) and polarization fading (polarization misalignment at receiver stage and polarization-induced phase noise [8]). A trade-off between spatial resolution and maximum reach arises, given that a high spatial resolution involves the use of narrow pulses resulting in a low signal to noise ratio (SNR). Increasing the energy of these pulses enhances the performance but also generates undesired non-linear effects. In order to further relax the spatial resolution versus maximum reach trade-off, our approach consists in continuously probing the sensor using coded sequences, instead of single pulses. The sequence is designed to optimize the covered mechanical bandwidth of the system and to guarantee a perfect channel estimation [7]. Moreover, instead of modulating one polarization state, we use polarization diversity by simultaneously probing two orthogonal polarization states. A dual-polarization coherent receiver is also used to detect the complete state of the Rayleigh backscattered field, hence mitigating polarization fading. Coherent fading is not tackled by the proposed technique. The conditions for achieving a perfect fiber impulse response estimation were studied in [7]. The desired phase information is extracted from Jones matrices computed up to a given location in the fiber.

We briefly describe the method in the following: the fiber is probed with two mutually orthogonal complementary binary pairs of Golay sequences $\{G_{a1}, G_{b1}\}$ and $\{G_{a2}, G_{b2}\}$ mapped to binary-phase-shift keying (BPSK) symbols (one bit per symbol $\{-1, 1\}$). The first pair $\{G_{a1}, G_{b1}\}$ modulates a given polarization state of the electric field (linear horizontal

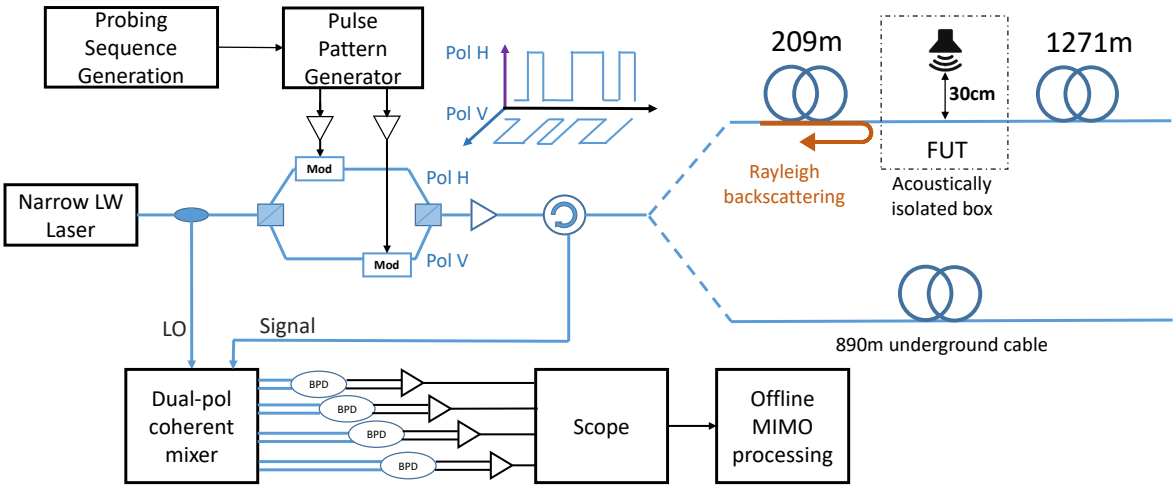

Fig. 1: Experimental setup of the interrogation scheme (BPD: Balanced photodiode, LW: Linewidth, MIMO: Multiple Input Multiple Output, Mod: Modulator, FUT: Fiber under test). Two sensing setups: a 1487m fiber and an 890m fiber cable.

for instance) while the second pair $\{G_{a2}, G_{b2}\}$ modulates a state that is orthogonal to the first (linear vertical). A basic example of mutually orthogonal complementary pairs is given by $G_{a1} = [1,-1,-1,-1], G_{b1} = [-1,1,-1,-1], G_{a2} = [-1,-1,1,-1], G_{b2} = [1,1,1,-1]$. Longer sequences can be obtained recursively from the above seed to get the desirable probing length. The duration of the probing code is defined as $T_{code} = \frac{2.(4.2^K)}{F_{symb}}$ where K is an integer standing for the number of recursions and F_{symb} stands for the symbol rate. The sensing fiber is continuously probed with a period T_{code} yielding a mechanical bandwidth $BW = 1/(2.T_{code})$. The native spatial step, or gauge length of a sensed fiber segment GL is equal to $c_f/(2F_{symb})$, where $c_f = c/n$ is the velocity of light in the SSMF core with refractive index $n \approx 1.45$ and c being the speed of light in vacuum.

B. Phase estimation and extraction of differential phases

At the receiver side, the Rayleigh backscattered signal from the i^{th} segment and at time index j (set by the j^{th} probing code) is given by: $\mathbf{E_r} = \mathbf{H_{i,j}}\mathbf{E_t}$ with $\mathbf{E_t}$ being the transmitted signal and $\mathbf{H_{i,j}}$ the dual-pass channel response up to segment i and at time index j represented by a 2×2 Jones matrix. The MIMO processing consists of four correlations between each of the two components of the emitted electrical field and the received electrical field respectively $\mathbf{E_t} = \{E_{tx}, E_{ty}\}$ and $\mathbf{E_r} = \{E_{rx}, E_{ry}\}$, in order to periodically compute the 2×2 Jones matrices at each T_{code}. The absolute dual-pass optical phase is then extracted from the Jones matrix as $\Phi = 0.5\angle\det(\mathbf{H_{i,j}})$ where $\det(\mathbf{H_{i,j}})$ stands for the determinant of $\mathbf{H_{i,j}}$. Being interested in the phase evolution per segment, we compute the differential phases $\Delta\phi$ by setting the absolute phase of the first fiber segment as a reference. The conditions for perfect estimation of $\mathbf{H_{i,j}}$ when the sensing fiber is probed with BPSK-mapped codes is $T_{code} > 4T_{ir}$ [7] where $T_{ir} = 2L/c_f$ stands for the time spreading of the channel response for a fiber of length L. The symbol rate and the code length are chosen accordingly to come up with a T_{code} value that complies with the above condition.

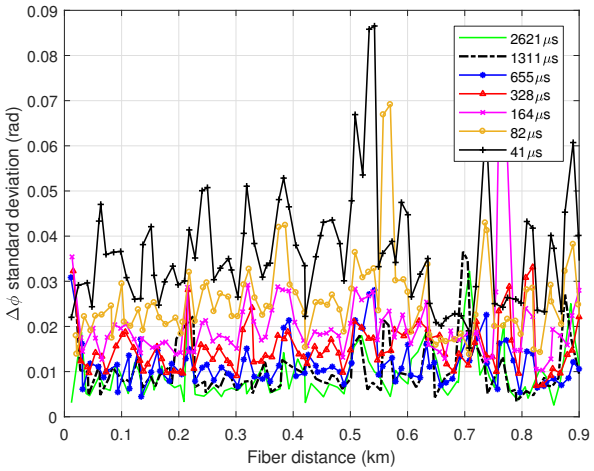

Fig. 2: Measured phase standard deviation (StDv) along 1km of fiber for different probing sequence lengths in static regime.

III. Experimental Setup

The interrogator and experimental setup is shown in Figure 1. A laser source with a 75Hz linewidth (observed during 1ms), emitting 11dBm at $\lambda = 1536$nm is used as a carrier and also serves as a local oscillator at the receiver side. The two BPSK-coded sequences modulate the carrier through a dual polarization Mach-Zehnder modulator (MZM) at 50MBaud. The signal is then sent through an optical amplifier and a circulator followed by two different fiber optic sensors configurations. A first setup consist in two SSMF spools of length 209m and 1271m respectively. A 5m-long 1mm-width tight buffered SSMF interconnects the two spools. The overall sensing fiber length is 1485m. The acoustic perturbation is applied on an 84cm-long section of the interconnecting fiber by means of a speaker located at 30cm in front of it. This fiber section and the speaker are acoustically isolated in a wooden box of size $82.5\text{cm} \times 84\text{cm} \times 204\text{cm}$ in order to attenuate the impact of disturbances from the surrounding environment that we cannot control (for instance fans in lab equipment and air conditioning) and ensure more reliable measurements. The

fiber section is tightly pulled and its two ends are attached on each side of the box. The second setup consists in using an existing underground fiber cable suspended on a metal track at a depth of 80cm below the floor level, containing 8 tight buffered fibers. It exits the lab and follows a long hallway before serving other labs. The overall length of the cable is 890m. We use the first 100m located under the hallway to detect perturbations. The backscattered signal is sent through a dual polarization coherent mixer consisting of two 90° optical hybrids. The in-phase and in-quadrature beating signals projected over two orthogonal polarization states are then captured by 1.7GHz balanced photodiodes. The resulting photocurrents are amplified through transimpedance amplifiers (TIAs) and captured on a 12bit-scope sampling at 100MSamples/s. The acquired data is then transferred on a PC for offline processing in order to extract Jones matrices as detailed in the previous section.

IV. Experimental Results

A. Static measurements

The longer the continuous probing sequences are, the higher the received SNR is. However, the smaller the covered mechanical bandwidth will be. Hence, the choice of the probing sequence length implies a trade-off between the noise reduction and the required bandwidth. In the first experiment, we study the influence of the sequence length on the estimated noise in static regime. Figure 2 shows the measured phase standard deviation (StDv) as a function of distance over a 1km fiber probed with code lengths T_{code} ranging from 41μs to 2621μs. The code length is varied by recursively generating codes using the seed sequences defined in section II, at a fixed symbol rate of 50MBaud. As we can see in Fig. 2, the higher the probing code length is, the lower is the phase StDv along the first kilometer. The high peaks in the phase StDv are due to the well-known coherent fading as we only tackle polarization fading with our MIMO interrogation scheme. The upper bound of the operational code length will be dictated by the coherence length of the laser [7]. When the code length exceeds this coherence length, a degradation of the phase StDv will be observed.

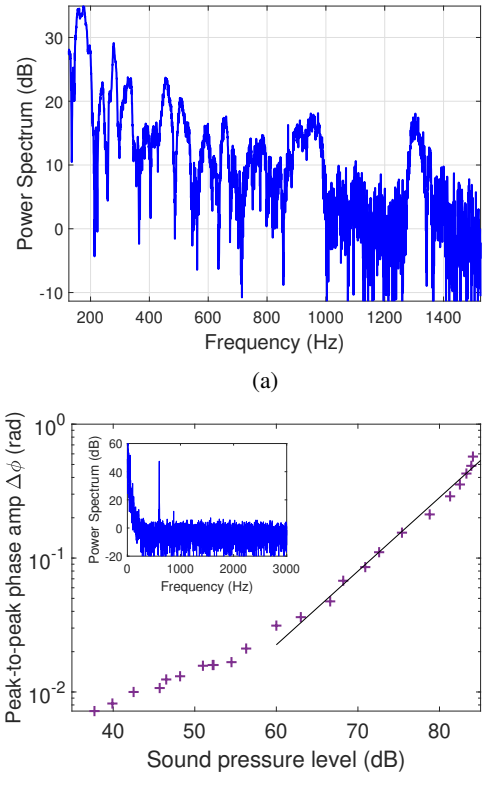

Fig. 3: (a) Power spectrum of $\Delta\phi$ for a linear frequency sweep $[100 : 1500]$Hz; (b) Peak-to-peak $\Delta\phi$ with respect to SPL for a 600Hz tone. Inset: power spectrum of $\Delta\phi$ for $\mathrm{SPL} = 85\mathrm{dB}$.

B. Dynamic measurements

Now, we focus on the ability of the interrogator to detect an acoustic signal. By using the first fiber setup shown in Fig. 1, we apply the acoustic perturbation by means of a speaker. First, we apply a frequency sweep covering the range $[100 : 1500]$Hz. We choose $T_{code} = 328\mu$s to guarantee the coverage of this bandwidth. Figure 3a shows the power spectral density (PSD) of the frequency sweep at the location of the perturbation. Notice that the frequency response is not at all linear but has maximum peaks as well as holes at different frequencies. This phenomenon can be explained given the configuration of the perturbed fiber section. Indeed, the fiber itself has an intrinsic linear response to strain as demonstrated in [7] but in the current configuration, the fiber section tightly stretched in a cavity acts as a resonator. If we take into account the resonance of the acoustic isolation box, the frequency modes will correspond to a coupling between the resonance of the fiber and the box. By computing the first frequency modes of the box used in the experiment [11], we notice that the peaks in Fig. 3a correspond to the resonance at these modes. Thus, the impact of the surrounding environment of the sensed fiber is important to grasp when performing acoustic measurements.

The next experiment aims at studying the sensitivity of the fiber at a given frequency. We generate a 600Hz tone chosen according to the resonance frequency modes found in the sweep experiment (see Fig. 3a) and record 0.2s-long acquisitions. To assess acoustic sensitivity, we measure and show in Fig. 3b the peak-to-peak phase amplitude as a function of the sound pressure level (SPL). The y-axis is in logarithmic scale. The SPL is referenced with respect to 20μPa (hearing threshold) and measured by means of a sound level meter located right behind the fiber section. Below an SPL of 60dB, a noise floor around $0.01\ \mathrm{rad_{pp}}$ appears due to ambient noise and self-noise of the interrogator. By doing a linear fitting of the experimental data, we compute an acoustic sensitivity of 0.13rad/dB. The PSD of the 600Hz tone is shown in the inset of Fig. 3b for $\mathrm{SPL} = 85\mathrm{dB}$.

We now examine the ability of the system to detect a speech signal in the same previous configuration. For this application, we choose to operate with a probing code of 164μs guaranteeing a coverage of a 3kHz bandwidth (standard voice frequency band in telephony). The signal delivered by the speaker is a 1s digitized voice signal "Bonjour". Figures 4a and 4b show the time-domain and spectrogram representations

of the original signal and the detected phase variations. In order to filter low frequency noise, we use a high pass filter with a cutoff frequency of 50Hz. Figure 4c displays the mean squared error (MSE) as a function of SPL in dB. The black square markers represent experimental data and the red line represents a polynomial interpolation. As expected, the MSE is decreasing as the speaker sound level increases. From 65dB (corresponding to a normal conversation level at a 1m distance), the MSE is lower than 4%, which corresponds to a well audible detected sound. Thus, with just a correlation process to extract the fiber response and from it the differential phases, it is possible to effectively recover a speech signal.

C. Field trial experiment

The following experiment consists in exploiting a deployed optical cable in our facilities (second fiber in Fig. 1) for vibration detection. Since low frequency signals are more likely to be detected in such configuration due to the propagation properties of mechanical waves through the ground, we focus on the detection of signals with frequencies lower than 700Hz. First, we gently hit the floor in the hallway at 70m from the interrogator, with a light weighted clothes rack, creating three impulses and repeat approximately each 2 seconds. We acquire signals during 10s and monitor the detected phase at 70m. The temporal phase variations are shown in Figure 5(a). As we can see, the detected signal is well retrieved. Then, we detect a person running from a distance of 70m to 30m from the lab. Figure 5(b) shows the space-time map of the received signal where the detected phase signals at different segments are shifted by their spatial location with respect to the interrogator (in meters). We can clearly see the steps all along the distance and compute the approximate running speed (4 m/s). Thus, it is possible to detect low frequency anthropogenic activities by using underground installed optical fiber cables.

V. Conclusion

We have proposed a polarization multiplexed coded phase-OTDR for acoustic perturbation detection solely from Rayleigh backscattering with 1mm tight buffered SSMF and an installed underground fiber cable. The detection of acoustic wave perturbations such as a speech signal with fair reliability has been successfully demonstrated. The ability of the system to detect acoustic signals with the use of underground installed optical fibers has been also demonstrated which paves the way for a wide range of applications on acoustic wave detection.

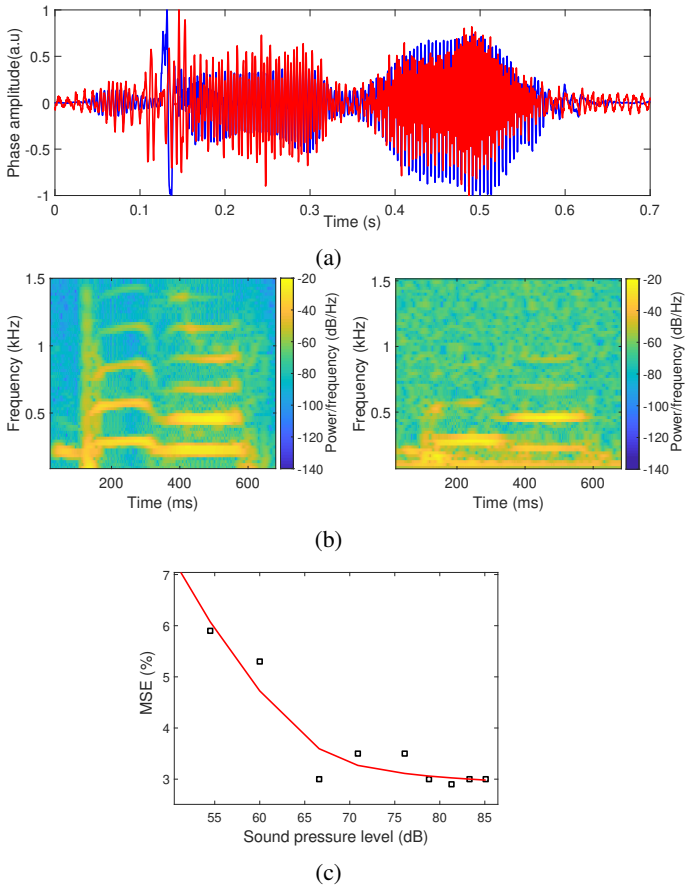

Fig. 4: Speech signal test: (a) Original signal (blue) and detected phase (red), (b) Spectrogram of original (left) and detected signal (right) (c) Mean squared error versus SPL.

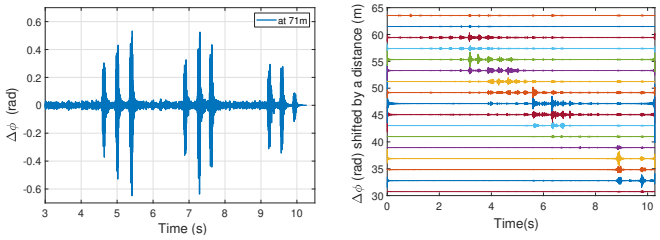

Fig. 5: (a) Phase variation when hitting the floor. (b) Space-time map of a 10-second running experiment.

References

[1] Y. Wu, J. Gan, Q. Li, et al., "Distributed Fiber Voice Sensor Based on Phase-Sensitive Optical Time-Domain Reflectometry," in *IEEE Photonics Journal*, vol. 7, no. 6, pp. 1-10, Dec. 2015.

[2] G. A. Wellbrock, T. J. Xia et al., "First Field Trial of Sensing Vehicle Speed, Density and Road Conditions by Using Fibre Carrying High Speed Data," Optical Fibre Conference, San Diego, March 2019.

[3] Arthur H. Hartog, "An Introduction to Distributed Optical Fibre", Chapter 6, Taylor & Francis Group, 2017.

[4] G. Yang, X. Fan, S. Wang, et al., "Long-range distributed vibration sensing based on phase extraction from phase-sensitive OTDR",in *IEEE Photonics Journal*, vol. 8, no 3, p. 1-12, 2016.

[5] H.F Martins, K. Shi, B.C Thomsen, et al., "Real time dynamic strain monitoring of optical link using the backreflection of live PSK data", in *Optics EXPRESS Journal*, vol.24, no.19, pp. 22303-22318, 2016

[6] M. Ren, P. Lu, L. Chen, X. Bao," Theoretical and Experimental Analysis of Phase-OTDR Based on Polarization Diversity Detection", in *IEEE Photonics Technology Letters*, vol. 28, no 6, pp. 697-700, 2016.

[7] Christian Dorize and Elie Awwad, "Enhancing the performance of coherent OTDR systems with polarization diversity complementary codes", in *Opt. Express*, OSA, Vol.26, pp. 12878-12890, May 2018.

[8] S. Guerrier et al., "Introducing coherent MIMO sensing, a fading-resilient, polarization-independent approach to Phase-OTDR," Opt. Express 28, 21081-21094, 2020.

[9] C. Dorize et al., "Vibration identification over 50km SSMF with Pol-Mux coded phase-OTDR", European Conference on Optical Communications, paper W.1.E.1, September 2019.

[10] C. Dorize et al., "Capturing Acoustic Speech Signals with Coherent MIMO Phase-OTDR", in proceedings of *ECOC*, paper We1A-7, 2020.

[11] H. Kuttruff, "Acoustics: An Introduction", Taylor& Francis, p.170, 2007.